PAPER

Simple Modeling of an Abdomen of Pregnant Women and Its Application to SAR Estimation

Hiroki KAWAI[†**a)], **Koichi ITO**[††], **Masaharu TAKAHASHI**[†††], **Kazuyuki SAITO**[†††], ***Members***,
Takuya UEDA[††††***], **Masayoshi SAITO**[††††], **Hisao ITO**[††††], **Hisao OSADA**[†††††****], ***Nonmembers***,
Yoshio KOYANAGI[†††,††††††], ***and*** **Koichi OGAWA**[†††,*], ***Members***

SUMMARY This paper presents a simple abdomen model of pregnant women and the evaluation of the specific absorption rate (SAR) inside the proposed model close to normal mode helical antennas (NHAs), which are replacing the portable radio terminals for business at 150 MHz. First, dielectric properties of amniotic fluid and those of fetus of rabbit, which have about the same electrical properties as human, are measured. As a result, the conductivity of amniotic fluid is 1.8 times and that of fetus is 1.3 times higher than that of adult muscle at 150 MHz. The result also suggests the modeling of pregnant women including the amniotic fluid and the fetus is necessary. Next, a simple abdomen model of pregnant women based on the measurements of magnetic resonance (MR) images of Japanese women in the late period of pregnancy is proposed. Finally, the SAR inside the proposed abdomen model close to 0.11λ and 0.18λ NHAs is calculated using the finite-difference time-domain (FDTD) method. As a result, we have confirmed that the 10-g average SAR in the fetus is sufficiently less than 2 W/kg, when the output power of NHAs is 5 W, which is the maximum power of portable radio terminals in Japan.
key words: *fetus, pregnant women, amniotic fluid, SAR, FDTD method*

1. Introduction

Radiofrequency (RF) devices, which are usually placed in the vicinity of human body, are widely used in various situations. For instance, pregnant women and their fetuses may be exposed to the electromagnetic (EM) waves radiated from the devices, such as portable radio terminals for business, induction heating (IH) cookers, hand-held metal detectors (HHMDs), etc. However, the EM dosimetry inside pregnant women and their fetuses has not investigated in sufficient detail. Therefore, the priority of EM dosimetry in fetuses is increasing [1]. Moreover, additional data on the dielectric and thermal properties of human tissues and organs at the foetal stage is also needed.

Until now, several papers on the evaluation of EM waves' exposure in the fetus have been published [2]–[4]. Fleming and Joyner [2] have demonstrated the SAR inside simple homogeneous and layered models by the plane wave's exposure in the early pregnancy (embryo) from 80–100 MHz, and in the late pregnancy (fetus) over the frequency range of 300–1500 MHz. Kainz et al. [3] have reported the induced current density and the SAR inside an abdomen model, which is composed by the external shape of pregnant woman in the 34th gestational week and a spherical fetus, close to a HHMD at 10 MHz. In these papers, the uterus was replaced by very simple models. However, the structure inside the models was not representative of actual situation due to the organ and tissue complexity of mother and fetus.

Kainz et al. [4] have presented the SAR and the temperature-rise inside an abdomen model, which is composed by the external shape [3] and a realistic uterus based on MR images (5 mm-resolution), close to 1.5 T (64 MHz) and 3 T (128 MHz) MR coils. However, little was known about the dielectric properties of amniotic fluid and those of fetus. Therefore, an abdomen model, which has an accurate structure, and actual dielectric properties of fetus are indispensable to evaluate the SAR of fetus.

Until now, high-resolution voxel ($\leq 2^3\,\text{mm}^3$) models, which are composed by various tissues, of head [5]–[7] and those of whole-body [8]–[10] based on MR images have been used. However, in pregnant women, the realization of high-resolution abdomen model using the images is difficult because the MR imaging are usually used to confirm a deformed child and not used for normal pregnancy. Here, the resolution of images in the body-axial direction is about 10 mm. Therefore, this paper presents a simple abdomen model, which is composed by only a few tissues, for both measurement and calculation.

Actual measurement of dielectric properties of human

Manuscript received December 13, 2005.
Manuscript revised May 17, 2006.
[†]The author is with the Graduate School of Science and Technology, Chiba University, Chiba-shi, 263-8522 Japan.
[††]The author is with the Faculty of Engineering, Chiba University, Chiba-shi, 263-8522 Japan.
[†††]The authors are with the Research Center for Frontier Medical Engineering, Chiba University, Chiba-shi, 263-8522 Japan.
[††††]The authors are with the Department of Radiology, Graduate School of Medicine, Chiba University, Chiba-shi, 260-8670 Japan.
[†††††]The author is with the Division of Maternal-Fetal Medicine, Department of Obstetrics and Gynecology, Chiba University Hospital, Chiba-shi, 260-8677 Japan.
[††††††]The author is with the Mobile Communication Technology Center, Panasonic Mobile Communications Co., Ltd., Yokosuka-shi, 239-0847 Japan.
[*]The author is with the Communication Devices Development Center, Matsushita Electric Industrial Co., Ltd., Kadoma-shi, 571-8501 Japan.
[**]Presently, with the National Institute of Information and Communications and Technology, Koganei-shi, 184-8795 Japan.
[***]Presently, with the Department of Radiology, Institute of Clinical Medicine, University of Tsukuba, Tsukuba-shi, 305-8575 Japan.
[****]Presently, with the Department of Obstetrics and Gynecology, Juntendo University Shizuoka Hospital, Izunokuni-shi, 410-2295 Japan.
a) E-mail: hkawai@m.ieice.org
DOI: 10.1093/ietcom/e89–b.12.3401

Copyright © 2006 The Institute of Electronics, Information and Communication Engineers

fetus is not normally possible. On the contrary, the electrical properties of mammals are almost equal to those of human [11]. Hence, we measure the dielectric properties of amniotic fluid and those of fetuses of rabbits, which are easier to obtain than those of human. In addition, the dielectric values of four organs of rabbit are also measured.

This paper presents a simple abdomen model of pregnant women and the evaluation of the SAR inside the proposed model at 150 MHz, which is commonly used in the portable radio terminals for business, e.g., police, broadcasting industry, fire fighting, security, etc. First, dielectric properties of internal organs, including the amniotic fluid and fetus, of rabbits are measured. Next, a simple abdomen model, which can be used for both measurement and calculation, based on the measurements of MR images of pregnant women in their late pregnancy is proposed. Finally, the SAR distribution and local SAR inside the proposed abdomen model close to 0.11λ and 0.18λ normal mode helical antennas (NHAs) [12]–[14], which are replacing the portable radio terminals at 150 MHz, are calculated using the FDTD method [15].

2. Measurement of Dielectric Properties of Internal Organs of Rabbit

2.1 Condition and Setting

In the measurement of dielectric properties, a Japanese white rabbit of twenty five days of pregnancy and eight fetuses are used. Here, the pregnancy of rabbit is almost equal to eight to nine months of pregnancy for the human because the measurement of dielectric properties of amniotic fluid and fetus is difficult in the early stage of pregnancy. In addition, the amount of amniotic fluid is the maximum in this period of pregnancy.

In the euthanasia of rabbits, a pentobarbital sodium solution was used. The euthanasia and dissection of rabbit were realized following a Guide for Animal Experimentation Inohana Campus, Chiba University, Chiba, Japan.

The measurement instrument of dielectric properties was an HP-85070M dielectric-probe measurement system manufactured by the Agilent Technology Co., Ltd., CA, USA. The temperature in the measurement room was 22°C. In addition, the humidity in the room was 32%. The temperature of internal organs was 22–24°C because of the stop of bloodstream by the death and the thermal diffusion by the death, ethanol cleaning, and air. All rat's tissues were used as fresh as possible, mostly within two hours after the death.

2.2 Results

2.2.1 Internal Organs

Figure 1 illustrates the measured dielectric properties of uterus, liver, muscle, and brain of rabbit and those of reference [11], which are widely used as the values of human tissues, over the frequency range from 100 MHz to 3 GHz. Uterus, liver, and muscle are selected because they are placed close to the amniotic fluid and the fetus. In addition, the values of brain are usually used as those of human head at cellular phones' frequencies. Here, we also confirm the dependence of these values of organs over this frequency range.

As shown in Figs. 1(a)–(d), the dielectric properties of tissues vs. the frequency are close to those of reference. Here, differences between the two are caused by the difference of frequency dispersiveness, e.g., relaxation time, static ionic conductivity, etc. [11].

From these results, we have confirmed that the electrical properties of this rabbit are almost equal to those of reference.

2.2.2 Amniotic Fluid and Fetus

Figure 2 shows measured dielectric properties of amniotic fluid of human and those of rabbit in the frequency range from 100 MHz to 3 GHz. Here, the amniotic fluid of human has been received from a Japanese healthy volunteer. Moreover, before the measurement, the amniotic fluids were centrifuged to separate the blood from the fluid. Figure 3 describes the measured dielectric properties of fetus of rabbit. The data are averages of measured values on the surface of head and abdomen, which are measurable points using the coaxial probe of 20 mm in diameter, of eight fetuses. Therefore, Fig. 3 also illustrates the maximum deviation from the average values.

As shown in Fig. 2, the dielectric properties of amniotic fluid of rabbit are close to the human data. Comparing Figs. 3 and 1(c), both the relative permittivity and conductivity of fetus of rabbit are higher than those of muscle, which are commonly used as the values of abdomen, of adult rabbit because of the difference of water content in the tissues. Peyman et al. [16] have also proposed the dielectric properties are due to the water content and the organic composition.

Comparing Figs. 2 and 3 with 1(c), the conductivity of amniotic fluid is 1.8 times and that of fetus is 1.3 times higher than that of adult muscle at 150 MHz. The results suggest the modeling of pregnant women including the amniotic fluid and the fetus is necessary.

Moreover, comparing Figs. 1 and 2, we have confirmed that the dielectric properties of organs of rabbit, which are placed around the fetus, are almost equal to those of human. Therefore, it is appropriate to use the values of fetus of rabbits instead of the human values. Here is an assumption that dielectric properties of adult human and rabbit are about the same, so therefore the values of human and rabbit fetuses are about the same.

3. Simple Abdomen Model of Pregnant Women

The SAR in the fetus is dependent on the pregnant term. The external shape of pregnant women is almost equal to non-pregnant women in the early stage of pregnancy (less

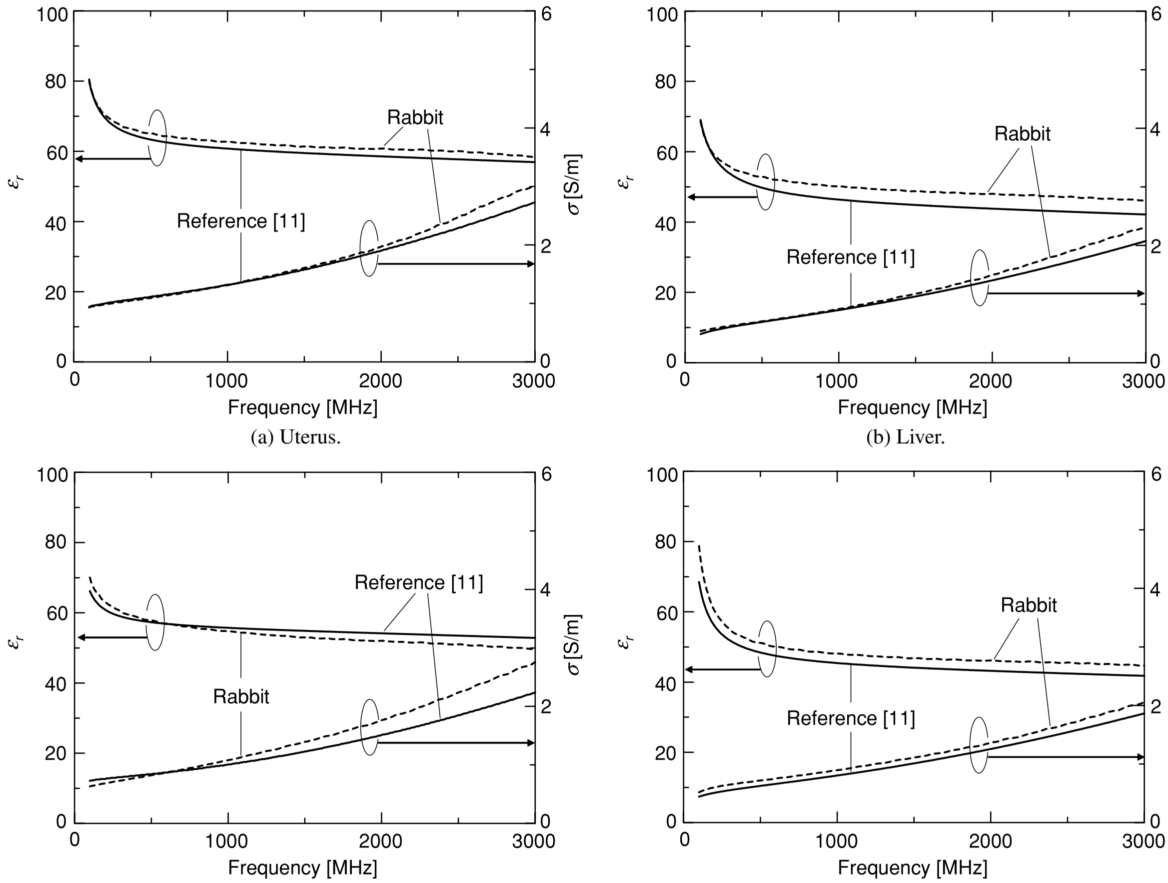

(a) Uterus. (b) Liver. (c) Muscle. (d) Brain.

Fig. 1 Measured dielectric properties of internal organs of rabbit and reference values over the frequency range of 100 MHz–3 GHz.

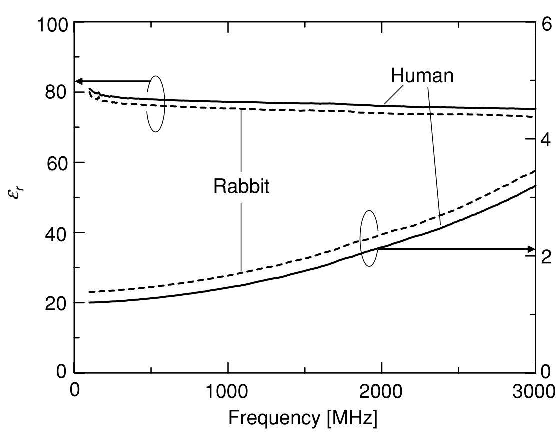

Fig. 2 Measured dielectric properties of amniotic fluid of human and those of rabbit over the frequency range of 100 MHz–3 GHz.

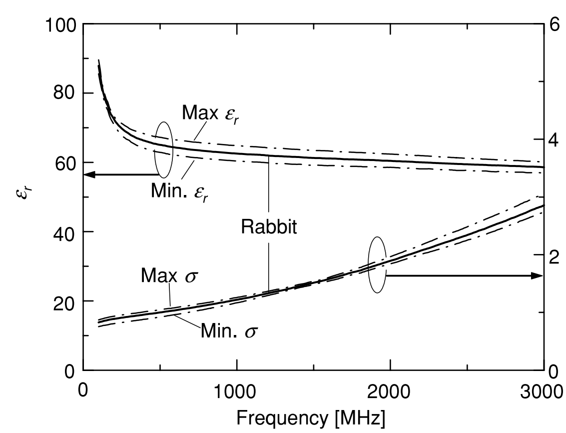

Fig. 3 Measured dielectric properties of fetus of rabbits over the frequency range of 100 MHz–3 GHz.

than 5 months). In addition, the measurement of dielectric properties of fetus of mammals in the early pregnancy is difficult. Moreover, the work of pregnant women is difficult in the very late period of pregnancy, which is above 9 months of pregnancy. Therefore, 6 to 8 months' pregnant women were chosen for examinations of MR imaging.

Twenty MR images, which were performed through the examinations of Japanese pregnant women in the Chiba University Hospital, Chiba, Japan, were reviewed for this modeling. However, the detailed modeling of pregnant woman using these images was difficult because the examinations were performed for clinical purposes so that they were usually performed about 10 mm intervals due to the time constraints in the pregnant condition. In addition, the definition of accurate average measurements inside the women is not normally possible. Moreover, the internal structure of pregnant women is dependent on their weight. Therefore, here is an assumption that the measurements based on MR images of middleweight women in the term are almost equal to average pregnant women.

Three images of Japanese middleweight (60–70 kg) pregnant women are used for the evaluation of measurements of tissues. Here, the weight is decided from the average pregnancy weight change among the term and the middleweight of non-pregnant female [17].

Figure 4 shows an example of MR image of a woman in her 30th gestational week. From three images, the measurements of maximum width, height, position of mothers' body, amniotic fluid, and fetus is evaluated.

Figure 5 illustrates a simple abdomen model, which can use both experiment and calculation, of pregnant women based on the average measurements of tissues. As shown in Fig. 5, the amniotic fluid and fetus are modeled by ellipsoids. Furthermore, the fetus is placed in the center of uterus because the position of fetus varies as times goes by. Additionally, the body axis of fetus is allocated along the vertical direction, to prevent the underestimate SAR in the fetus. Here, these ellipsoids have about the same volume as the real amniotic fluid and fetus. In addition, the summation of the SAR in the fetus using this model may be larger than that of realistic model because the curvature of this fetus is less than that of abdomen of real fetus. Moreover, the mother's body is replaced by a homogeneous cylindroid because realizing the complex structure around the uterus is difficult in the experiment. Furthermore, the height of abdomen model is 500 mm because the maximum value and distribution of the SAR in the model is almost equal to that in the whole-body model [13].

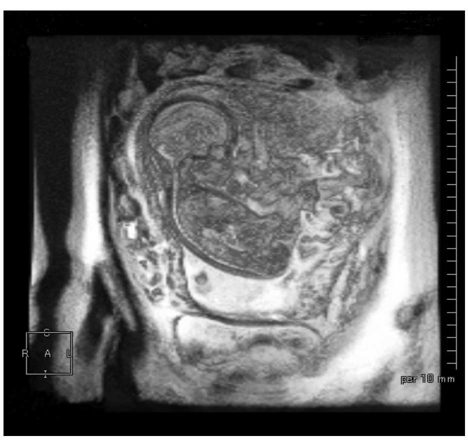

Fig. 4 Example of MR image of pregnant woman in the 30th gestational week.

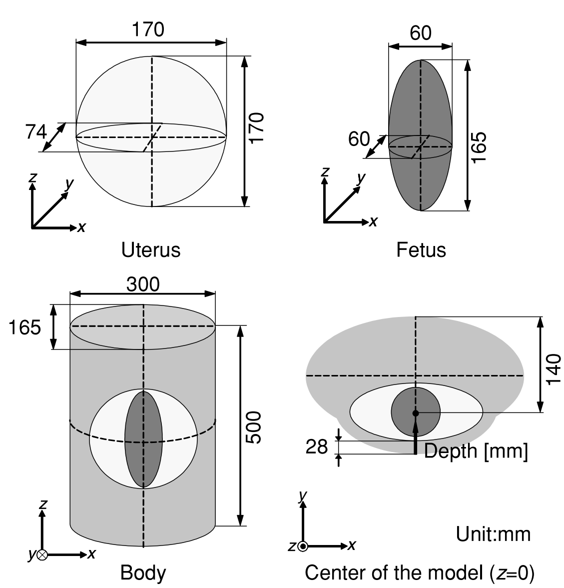

Fig. 5 Simple abdomen model of pregnant women.

4. Evaluation of the SAR Inside a Simple Abdomen Model of Pregnant Women

4.1 Numerical Model

Figure 6 shows the numerical model. In this paper, the NHAs simulate the actual portable radio terminals at 150 MHz, which are composed by a monopole NHA and a small radio box, because the SAR measurement using the thermographic method needs high power (above dozens of watts) [13], [14]. The structure and characteristics of NHAs have been studied in sufficient detail [12]. Moreover, the validity of replacement of the NHAs has been presented [14].

These NHAs are conjugate-matched by a capacitor. From now on, the antennas are called ANT1 and ANT2. The parameters of ANT1 (pitch S [mm], number of windings N, winding diameter $2R$ [mm], and axial length L [mm]) are as follows; $L = 212$ mm (0.11λ), $N = 38.4$, $2R = 15$ mm, $S = 5.4$ mm. In addition, those of ANT2 are as follows; $L = 356$ mm (0.18λ), $N = 99$, $2R = 7.5$ mm, $S = 3.4$ mm. Here, the $2R$ of ANT1 is twice of that of ANT2 to improve the ohmic loss. The diameter of metal wire is 1.0 mm. The measured efficiency of NHAs in free space is −1.4 dB (ANT1) and −1.2 dB (ANT2).

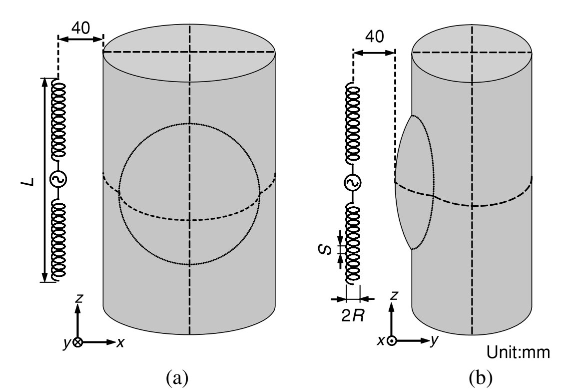

Fig. 6 Models for calculation. (a) Side position (normal case). (b) Front position (close to the fetus).

Table 1 Dielectric properties and density of tissues at 150 MHz.

Tissue	Body	AF	Fetus
ε_r	42.1	79.6	77.0
σ [S/m]	0.51	1.21	0.86
ρ [kg/m^3]	1,000	1,000	1,000

AF: Amniotic fluid

Figure 6(a) illustrates an evaluation model of normal case, when the NHAs are placed on the side of simple abdomen model. Figure 6(b) presents an evaluation model, when the NHAs are placed in front of the model. In addition, the distance between the antenna and the surface of model is 40 mm, which is the average distance between five real devices and the abdomen including the thickness of holder and wear. The effect of the distance on the SAR in the fetus is shown in Appendix. Moreover, the origin is the feed point of antennas.

4.2 Numerical Condition

The FDTD software (SEMCAD ver. 1.6, build 110, by Schmid & Partner Engineering AG, Zürich, Switzerland†) was used for the SAR calculating in the abdomen model. The parameters of FDTD calculation employed in this paper were as follows. The cell size of NHAs was 0.5–1 mm, abdomen model was 0.5–5 mm, and free space was 0.5–20 mm. Spacing ratio between non-uniform cells is 1.5. Here, the helical structure of antennas was precisely modeled using the voxels. The computational domains are $340 \times 300 \times 540\,\mathrm{mm}^3$ ($119 \times 158 \times 462$ cells) on the side position and $380 \times 320 \times 540\,\mathrm{mm}^3$ ($146 \times 97 \times 462$ cells) on the front position. In addition, the absorbing boundary condition was the perfectly matched layer (PML) (eight layers). Moreover, the calculation time was 30 (ANT1) or 25 (ANT2) periods at 150 MHz to get converged results.

Table 1 describes the dielectric properties and density of three tissues at 150 MHz. The values of the mother's body are 2/3 of those of muscle, which are generally used as the mixture of whole-body tissues [20] because the body is mainly composed by the fat and muscle in front of uterus. Here, the electrical properties of amniotic fluid are measured values of human [see Fig. 2]. In addition, the values of fetus are measured values of rabbit [see Fig. 3].

4.3 Results

4.3.1 SAR Distribution

Figure 7 shows the calculated SAR distributions inside the abdomen model on the $x-y$ plane ($z = 0$) [see Fig. 5 (right-under)] when the antennas are placed on the side of model. From now on, the input power of antennas is normalized to 1.0 W. Here, the output power of antennas is corrected by the efficiency in free space, as expressed in 4.1.

Comparing Fig. 7(a) and (b), the peak SAR of ANT1 is higher than that of ANT2 because the current locality of ANT1 is higher than that of ANT2. In addition, the SAR in the fetus is hardly obtained in both models because the value in the fetus is attenuated by the distance from the surface. Moreover, the SAR in the fetus region is very smaller than that in the body region.

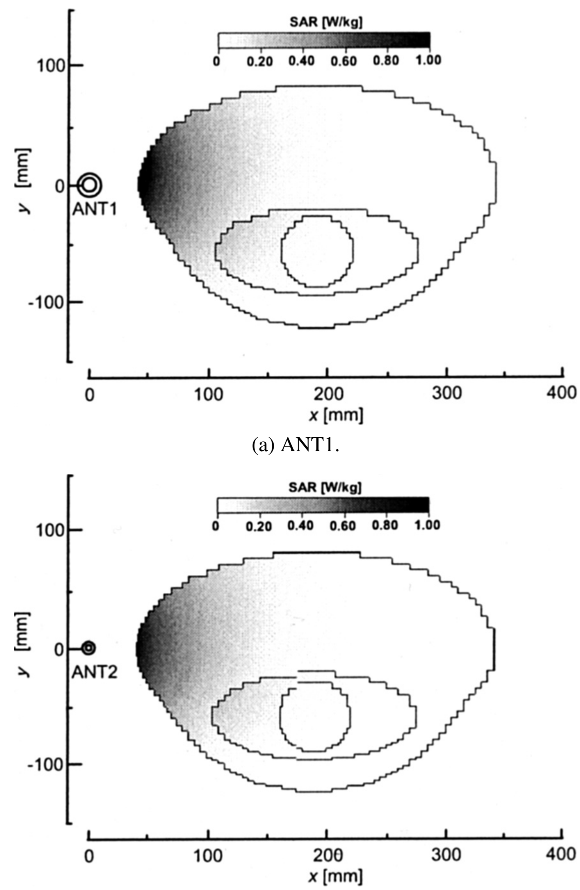

(a) ANT1.

(b) ANT2.

Fig. 7 SAR distributions on the $x-y$ plane ($z = 0$, side position).

Figure 8 illustrates the calculated SAR distributions inside the model on the $x-y$ plane ($z = 0$) when the antennas are placed in front of the model.

As shown in Fig. 8(a), the SAR distribution in the model by ANT1 is asymmetrical on the x direction because the SAR is generated by horizontal and vertical currents on the NHA. Here, the asymmetry by ANT1 is larger than that by ANT2 because the winding diameter of ANT1 is larger than that of ANT2. In addition, from Figs. 8(a) and (b), a high SAR distribution in the amniotic fluid region is obtained because the conductivity of amniotic fluid is almost 2.4 times higher than that of body, as expressed in Table 1. The results also show the variation in the SAR distribution around the boundary of tissues.

Figure 9 shows the calculated SAR distribution on the observational line ($x = z = 0$) [see Fig. 5 (right-under)] when the NHAs are placed in front of the model. Here, the SAR distribution of homogeneous model, which is composed by the body-equivalent tissue, is also calculated to

†[Online]. Available: http://www.speg.com/

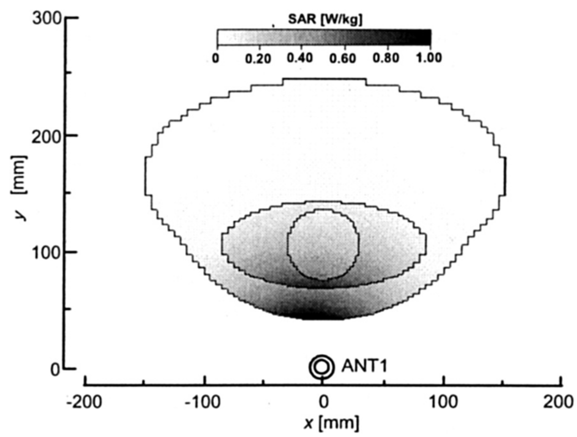

(a) ANT1.

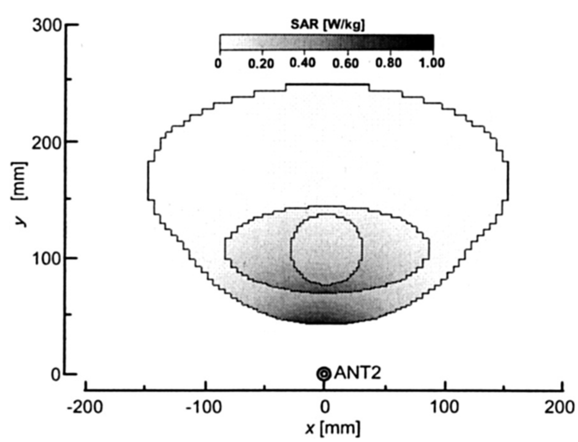

(b) ANT2.

Fig. 8 SAR distributions on the $x - y$ plane (z = 0, front position).

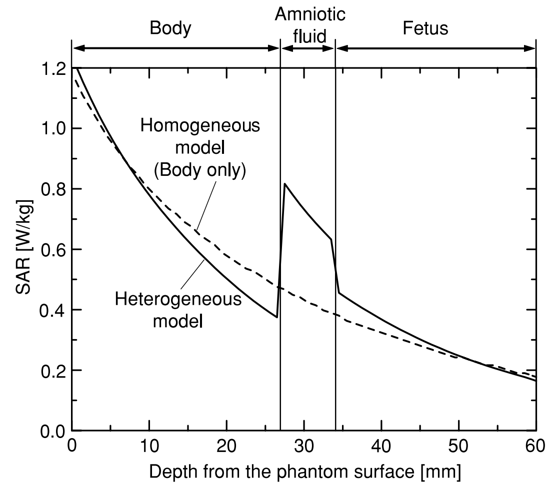

(a) ANT1.

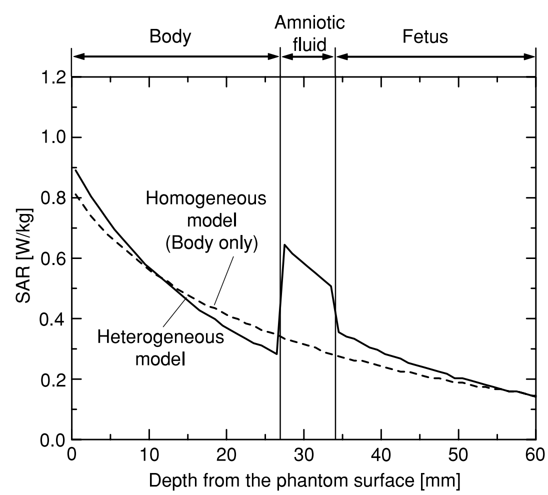

(b) ANT2.

Fig. 9 SAR distributions on the observational line (x = z = 0, front position).

evaluate the effect of heterogeneous structure on the distribution.

As shown in Figs. 9(a) and (b), it is confirmed that the attenuation of the SAR in the body is abruptly varied by the heterogeneous structure. In addition, the distribution inside the model suddenly varies around the boundary of tissues because the difference of conductivity between the tissues is very large, as expressed in Table 1. Moreover, the SAR ratio between the body and fetus region by ANT1 (0.11λ) is larger than that by ANT2 (0.18λ), because the locality of current distribution in the z direction of ANT2 is lower than that of ANT1. Here, the diffraction of E-field in the z direction, which is dependent on the current distribution, of ANT2 is higher than that of ANT1.

4.3.2 Average SAR

Figure 10 illustrates the calculated local 10-g average SAR in the mother and that in the fetus.

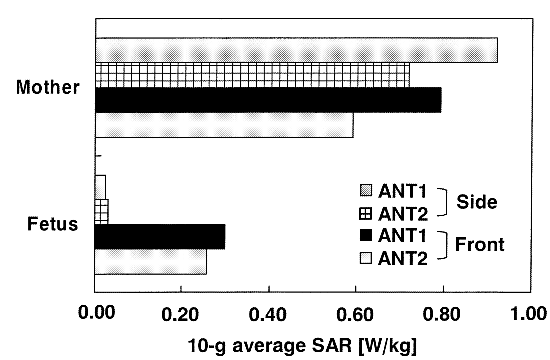

Fig. 10 Local 10-g average SAR.

As shown in Fig. 10, it is indicated that the EM waves hardly penetrate into the fetus, when the antennas are placed on the side. On the other hand, the average SAR in the fetus at the front position is almost 10 times larger than that at the side position. In addition, the result also suggests the local 10-g average SAR in the fetus is less than 1.50 W/kg, when the input power of NHAs is 5 W, which is the maximum power of 150 MHz portable radio terminals for business in Japan. Here, the input impedance of NHAs is perfectly matched close to the abdomen model. It is assumed that the SARs are strongly reduced by the mismatch loss, which is caused by the vicinity of human body, e.g., 9.5 dB when the ANT2 is placed in the same position [12]. From these results, the local 10-g average SAR in the fetus is sufficiently less than 2 W/kg, which is the non-occupational limit in Japan [21].

5. Conclusion

In this paper, the simple abdomen model of pregnant women and the evaluation of the SAR inside the proposed model, which was placed close to two types of NHAs, were proposed at 150 MHz.

The important findings in this paper are as follows.

1) The dielectric properties of amniotic fluid and those of fetus of rabbit were measured. The result had suggested the modeling of pregnant women including the amniotic fluid and fetus was necessary. Next, the simple abdomen model, which was composed by three types of tissues (body, amniotic fluid, fetus), based on measurements of MR images of Japanese pregnant women in late pregnancy was introduced.

2) The SAR distribution in the abdomen model was calculated using the FDTD method when the NHAs were placed in front or side of the model. As a result, the SAR ratio between the body and fetus region by ANT1 (0.11λ) was larger than that by ANT2 (0.18λ) because the diffraction of E-field in the z direction of ANT2 was larger than that of ANT1. Moreover, the SAR distribution around the boundary of amniotic fluid was abruptly varied by the heterogeneous structure when the antennas were placed in front of the model.

3) The average SAR in the model was also investigated. As a consequence, the 10-g average SAR in the fetus was sufficiently less than 2 W/kg, when the output power of NHAs is 5 W, which is the maximum power of portable radio terminals in Japan.

In the near future, we will measure the SAR distribution in the simple abdomen phantom. In addition, a more precision modeling of pregnant women will be investigated.

Acknowledgments

The authors would like to thank the members of the Technical Committee on Human Phantoms for Electromagnetics, IEICE, Japan, for their advice concerning this study.

References

[1] WHO, "Children's EMF research agenda," The International EMF Project, June 2004.

[2] A.H.J. Fleming and K.H. Joyner, "Estimates of absorption of radiofrequency radiation by the embryo and fetus during pregnancy," Health Phys., vol.63, no.2, pp.149–159, Aug. 1992.

[3] W. Kainz, D.D. Chan, J.P. Casamento, and H.I. Bassen, "Calculation of induced current densities and specific absorption rates for pregnant women exposed to hand-held metal detectors," Phys. Med. Biol., vol.48, pp.2551–2560, Aug. 2003.

[4] W. Kainz, T.R. Kellon, R. Qiang, and J. Chen, "Development of pregnant woman models for nine gestational ages and calculation of fetus heating during magnetic resonance imaging (MRI)," Proc. 27th BEMS and EBEA meeting, (CD-ROM), no.12-3, pp.137–139, Dublin, Ireland, June 2005.

[5] O.P. Gandhi, G. Lazzi, and C.M. Furse, "Electromagnetic absorption in the human head and neck for mobile telephones at 835 MHz and 1900 MHz," IEEE Trans. Microw. Theory Tech., vol.44, no.10, pp.1884–1897, Oct. 1996.

[6] F. Schoenborn, M. Burkhardt, and N. Kuster, "Difference in energy absorption between heads of adults and children in the near field of sources," Health Phys., vol.74, no.2, pp.160–168, Feb. 1998.

[7] J. Wang and O. Fujiwara, "Comparison and evaluation of electromagnetic absorption characteristics in realistic human head models of adult and children for 900-MHz mobile telephones," IEEE Trans. Microw. Theory Tech., vol.51, no.3, pp.966–971, March 2003.

[8] P.A. Mason, W.D. Hurt, T.J. Walters, J.A. D'Andrea, P. Gajšek, K.L. Ryan, D.A. Nelson, K.I. Smith, and J.M. Ziriax, "Effects of frequency, permittivity, and voxel size on predicted specific absorption rate values in biological tissue during electromagnetic-field exposure," IEEE Trans. Microw. Theory Tech., vol.48, no.11, pp.2050–2057, Nov. 2000.

[9] T. Nagaoka, S. Watanabe, K. Sakurai, E. Kunieda, S. Watanabe, M. Taki, and Y. Yamanaka, "Development of realistic high-resolution whole-body voxel models of Japanese adult males and females of average height and weight, and application of models to radio-frequency electromagnetic-field dosimetry," Phys. Med. Biol., vol.49, pp.1–15, 2004.

[10] P. Dimbylow, "Development of the female voxel phantom, NAOMI, and its application to calculations of induced current densities and electric fields from applied low frequency magnetic and electric fields," Phys. Med. Biol., vol.50, pp.1047–1070, 2005.

[11] C. Gabriel, "Compilation of the dielectric properties of body tissues at RF and microwave frequencies," Brooks Air Force Technical Report, AL/OE-TR-1996-0037, 1996.

[12] K. Ogawa, Y. Koyanagi, and K. Ito, "An analysis of the effective radiation efficiency of the normal mode helical antenna close to the human abdomen at 150 MHz and consideration of efficiency improvement," Electron. Commun. Jpn. 1. Commun., vol.85, no.8, pp.23–33, 2002.

[13] Y. Koyanagi, H. Kawai, K. Ogawa, and K. Ito, "Internal distribution of the local SAR in the human abdomen measured by a split phantom and small helical antennas at 150 MHz," Proc. Int. IEEE Antennas and Propagation Symp., vol.3, pp.1079–1082, Columbus, USA, June 2003.

[14] Y. Koyanagi, H. Kawai, K. Ogawa, and K. Ito, "Estimation of the local SAR in the human abdomen using a human body phantom and small antennas at 150 MHz," IEICE Trans. Commun. (Japanese Edition), vol.J86-B, no.7, pp.1207–1218, July 2003.

[15] K.S. Yee, "Numerical solution of initial boundary value problems involving Maxwell's equation in isotropic media," IEEE Trans. Antennas Propag., vol.14, no.3, pp.302–307, March 1966.

[16] A. Peyman, A.A. Rezazadeh, and C. Gabriel, "Changes in the dielectric properties of rat tissue as a function of age at microwave frequencies," Phys. Med. Biol., vol.46, pp.1617–1629, June 2001.

[17] H. Murooka, S. Takeuchi, and K. Iwasaki, ed., The lifelong obstetrics and gynecology science, vol.2, Kanehara, Tokyo, 1984.

[18] A.W. Guy, "Analysis of electromagnetic fields induced in biological tissues by the thermographic studies on equivalent phantom models," IEEE Trans. Microw. Theory Tech., vol.19, no.2, pp.205–214, Feb. 1971.

[19] Y. Okano, K. Ito, I. Ida, and M. Takahashi, "The SAR evaluation method by a combination of thermographic experiments and biological tissue-equivalent phantoms," IEEE Trans. Microw. Theory Tech., vol.48, no.11, pp.2094–2103, Nov. 2000.

[20] A.W. Guy, C.-K. Chou, and B. Neuhaus, "Average SAR and SAR distributions in man exposed to 450-MHz radiofrequency radiation,"

IEEE Trans. Microw. Theory Tech., vol.32, no.8, pp.752–762, Aug. 1984.
[21] "Radio-radiation protection guidelines for human exposure to electromagnetic fields" (in Japanese), Telecommun. Technol. Concil Ministry Posts Telecommun., Deliberation Rep. 89, Tokyo, Japan, 1997.
[22] Supplement C to bulletin 65, Evaluating compliance with FCC guidelines for human exposure to radiofrequency electromagnetic fields, 2001.

Appendix: Effect of Distance between the Antenna and the Abdomen Model on the SAR in the Fetus

In this paper, the distance between the NHAs and the surface of abdomen model was fixed at 40 mm. However, in the actual situation, the distance is easily varied. Moreover, the variation in the distance causes the variation in the SAR and input impedance. Therefore, this appendix presents the effect of distance between the NHA and the abdomen on the SAR in the fetus, when the NHA is placed in front of the abdomen.

ANT2 and an abdomen model [see Section 4.1] were used, because the dependence of mismatch loss of ANT2 on the distance was already proposed [12]. Here, the distance was varied at 25 mm, which was the distance of two way radio in the compliance test [22], 40 mm, and 55 mm. Table A· 1 describes the mismatch loss of ANT2 vs. distance [12].

Figure A· 1 shows the calculated result of local 10-g average SARs in the fetus plotted against the distance. Here, the input power of ANT2 was normalized to 1.0 W. In the mismatch results, the mismatch losses in each distance [see Table A· 1] were corrected.

Table A· 1 Mismatch loss vs. distance between ANT2 and the abdomen model.

Distance [mm]	Mismatch loss [dB]
25	11.5
40	9.5
55	8.0

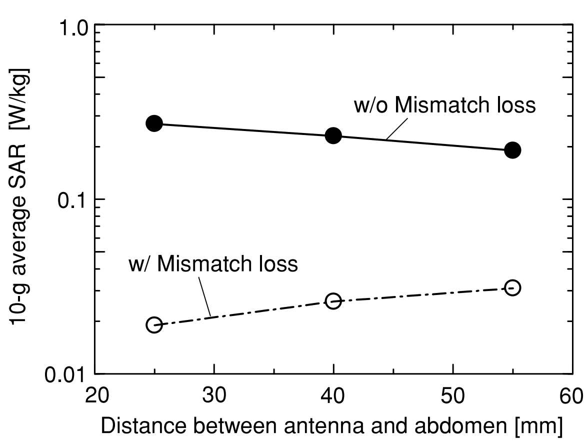

Fig. A· 1 Local 10-g average SAR in the fetus vs. distance between ANT2 and the abdomen model.

As shown in Fig. A· 1, in the matching condition, the increase in the SAR is proportional to the decrease in the distance. However, in the mismatch condition, the maximum SAR is arisen at 55 mm. Therefore, these results suggest that the proximity of antenna does not necessarily generate the worst SAR in the fetus by the mutual coupling.

Hiroki Kawai was born in Chiba, Japan, on March 1977. He received the B.E., M.E., and D.E. degrees all in electrical engineering from Chiba University, Chiba, Japan, in 1999, 2001, and 2005 respectively. He is currently an Expert Researcher at National Institute of Information and Communications Technology, Tokyo, Japan. His main interests include analysis and design of small antennas using animal study, research on evaluation of the interaction between electromagnetic fields and the human body using numerical and experimental phantoms. Dr. Kawai is a member of the IEEE and the BEMS.

Koichi Ito was born in Nagoya, Japan, in June 1950. He received the B.S. and M.S. degrees from Chiba University, Chiba, Japan, in 1974 and 1976, respectively, and the D.E. degree from Tokyo Institute of Technology, Tokyo, Japan, in 1985, all in electrical engineering. From 1976 to 1979, he was a Research Associate at Tokyo Institute of Technology. From 1979 to 1989, he was a Research Associate at Chiba University. From 1989 to 1997, he was an Associate Professor at the Department of Electrical and Electronics Engineering, Chiba University, and is currently a Professor at the Faculty of Engineering, Chiba University. He has been appointed as one of the Deputy Vice-Presidents for Research, Chiba University since April 2005. In 1989, 1994, and 1998, he visited the University of Rennes I, France, as an Invited Professor. Since 2004 he has been appointed as an Adjunct Professor to Institute of Technology Bandung (ITB), Indonesia. His main research interests include analysis and design of printed antennas and small antennas for mobile communications, research on evaluation of the interaction between electromagnetic fields and the human body by use of numerical and experimental phantoms, and microwave antennas for medical applications such as cancer treatment. Professor Ito is a Fellow of the IEEE, and a member of AAAS, the Institute of Image Information and Television Engineers of Japan (ITE) and the Japanese Society of Hyperthermic Oncology. He served as Chair of Technical Group on Radio and Optical Transmissions of ITE from 1997 to 2001 and Chair of Technical Group on Human Phantoms for Electromagnetics, IEICE from 1998 to 2006. He also served as Chair of the IEEE AP-S Japan Chapter from 2001 to 2002 and TPC Co-Chair of the International Workshop on Antenna Technology (IWAT) 2006 which was held in New York, USA, in 2006. He is now Vice-Chair of the 2007 International Symposium on Antennas and Propagation (ISAP2007) to be held in Niigata, Japan. He has served as an Associate Editor of IEEE Transactions on Antennas and Propagation since 2004 and as a Distinguished Lecturer for the IEEE Antennas and Propagation Society since 2006.

Masaharu Takahashi was born in Chiba, Japan, on December 15, 1965. He received the B.E. degree in electrical engineering in 1989 from Tohoku University, Miyagi, Japan, and the M.E. and D.E. degrees both in electrical engineering from Tokyo Institute of Technology, Tokyo, Japan, in 1991 and 1994 respectively. He was a Research Associate from 1994 to 1996, an Assistant Professor from 1996 to 2000 at Musashi Institute of Technology, Tokyo, Japan, and an Associate Professor from 2000 to 2004 at Tokyo University of Agriculture and Technology, Tokyo, Japan. He is currently an Associate Professor at the Research Center for Frontier Medical Engineering, Chiba University, Chiba, Japan. His main interests have been electrically small antennas, planar array antennas, and electromagnetic compatibility (EMC). He received the IEEE Antennas and Propagation Society (IEEE AP-S) Tokyo chapter young engineer award in 1994. He is a member of the IEEE.

Kazuyuki Saito was born in Nagano, Japan, in May 1973. He received the B.E., M.E. and D.E. degrees all in electronic engineering from Chiba University, Chiba, Japan, in 1996, 1998, and 2001, respectively. He is currently a Research Associate with the Research Center for Frontier Medical Engineering, Chiba University. His main interest is in the area of medical applications of the microwaves including the microwave hyperthermia. He received the IEICE AP-S Freshman Award, the Award for Young Scientist of URSI General Assembly, the IEEE AP-S Japan Chapter Young Engineer Award, the Young Researchers' Award of IEICE, and the International Symposium on Antennas and Propagation (ISAP) Paper Award in 1997, 1999, 2000, 2004, and 2005 respectively. Dr. Saito is a member of the IEEE, the Institute of Image Information and Television Engineers (ITE), Japan, and the Japanese Society of Hyperthermic Oncology.

Takuya Ueda was born in Aomori, Japan, on August 1968. He received the M.D. and Ph.D. degrees both in medicine from Chiba University, Chiba, Japan in 1994 and 2004, respectively. From 1994 to 2003, he was a Clinical Fellow at the Chiba University Hospital, Japan. From 2004 to 2005, he was a Teaching Staff at the Graduate School for Medicine, Chiba University, Japan. He is currently an Assistant Professor at the Institute of Clinical Medicine, University of Tsukuba, Ibaraki, Japan. His main interest has been diagnostic radiology. Dr. Ueda is a member of the Radiological Society of North America, Japan Radiological Society, and Japanese Society for Magnetic Resonance in Medicine.

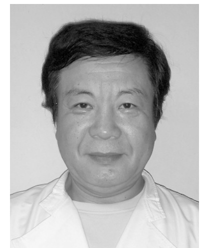

Masayoshi Saito was bone in Hokkaido, Japan, on July 1948. He received the B.E. degree in agriculture and Ph.D. degree in veterinary medicine from Nippon Veterinary and Animal Science University, Tokyo, Japan in 1972 and 2006, respectively. From 1986 to 2001, he was a Teaching Staff at the Institute for Training Radiological Technicians Affiliated to Chiba University School of Medicine, Chiba, Japan. He is currently a Staff of Research at the Department of Radiology, Faculty of Medicine, Chiba University, Chiba, Japan. Dr. Saito is a member of the Japanese Association for Laboratory Animal Science and the Japan Radiation Research Society.

Hisao Ito was born in Kanagawa, Japan, on April 1945. He received the M.D. and Ph.D. degrees both in medicine from Keio University, Tokyo, Japan in 1970 and 1978, respectively. From 1970 to 1977, he was a Research Associate at the Department of Gynecology, Keio University Hospital, Tokyo, Japan. He was a Research Associate from 1978 to 1979, an Assistant Professor from 1980 to 1989, and an Associate Professor from 1990 to 1995 at the Department of Radiology, Keio University Hospital. In 1981–1983, 1988, and 1990, he stayed at the Division of Radiation Therapy, M.D. Anderson Cancer Center, University of Texas, USA, as a Visiting Scientist. He is currently a Professor and Chair at the Department of Radiology, Faculty of Medicine, Chiba University, Chiba, Japan. His main interests include modification of radiation therapy and protection of the normal tissue from radiation damage.

Hisao Osada was born in Kanagawa, Japan, on June 1955. He received the M.D. and Ph.D. degrees both in medicine from Chiba University, Chiba, Japan in 1981 and 1991, respectively. From 1981 to 1982, he was a Resident in Obstetrics and Gynecology, Chiba University Hospital, Chiba, Japan. From 1982 to 1984, he was a Resident in Obstetrics and Gynecology, Kimitsu Central Hospital, Chiba, Japan. From 1984 to 1985, he was a Resident in Obstetrics and Gynecology, Chiba University Hospital. From 1987 to 1990, he was a Postdoctoral Fellow in Genetics, Stanford University School of Medicine, California, USA. From 1991 to 1998, he was an Instructor of Obstetrics and Gynecology, Chiba University School of Medicine. From 1998 to 2004, he was an Assistant Professor, Department of Obstetrics and Gynecology, Chiba University Hospital. From 2004 to 2005, he was a Director of Division of Maternal-Fetal Medicine, Department of Obstetrics and Gynecology, Chiba University Hospital. He is currently an Assistant Professor, Department of Obstetrics and Gynecology, Juntendo University Shizuoka Hospital.

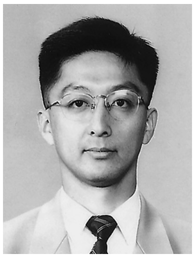

Yoshio Koyanagi was born in Tokyo, Japan, on August 21, 1965. He received a B.S. degree in communication engineering from The University of Electro-Communications of Japan in 1989, and a Ph.D. degree in engineering from Chiba University, Chiba, Japan in 2003. Since 1989 he has been with Matsushita Communication Industrial Co., Ltd. And is currently a leader of the RF project for 3G-LTE mobile phone in Communication System Development Center, Panasonic Mobile Communications Co.,Ltd, Yokosuka, Japan. His research is concerned with mobile handset antennas and MIMO antennas and EM biological effects. He is a member of IEEE. He is listed in Who's Who in the World.

Koichi Ogawa was born in Kyoto, Japan, on May 28, 1955. He received the B.S. and M.S. degrees both in electrical engineering from Shizuoka University, Shizuoka, Japan in 1979 and 1981, respectively. He received the Ph.D. degree in electrical engineering from Tokyo Institute of Technology, Tokyo, Japan, in 2000. He joined the Matsushita Electric Industrial Co., Ltd., Osaka, Japan in 1981, where he was engaged in research and development work on a millimeter-wave integrated circuit and various key components for cellular radio, which include antennas, filters, amplifiers and oscillators, etc. He is currently a Research Group Leader of Mobile Communication RF-Devices. His research interests include compact antennas, diversity/adaptive array antennas for mobile communication systems, electromagnetic interaction between antennas and a human body, and other related areas of radio propagation. His research also includes millimeter-wave circuitry and radio propagation. He received the OHM Technology Award from the Promotion Foundation for Electrical Science and Engineering in 1990, based on accomplishments and contributions to millimeter-wave technologies. He also received the TELECOM System Technology Award from the Telecommunications Advancement Foundation (TAF) in 2001, based on accomplishments and contributions to portable handset antenna technologies. Dr. Ogawa is the chief director of a technical committee for the Next Generation Wireless Communications in the Kansai Electronic Industry Development Center (KEC), Osaka, Japan. From 2003 he has been engaged as a Guest Professor of the Research Center for Frontier Medical Engineering, Chiba University, Chiba, Japan. He is a senior member of the IEEE. He is listed in Who's Who in the World.